Limnol. Oceanogr., 52(1), 2007, 217–229

Optical properties of the "clearest" natural waters

André Morel, Bernard Gentili, Hervé Claustre, Marcel Babin, Annick Bricaud, Joséphine Ras, and Fanny Tièche
Laboratoire d'Océanographie de Villefranche, Université Pierre et Marie Curie and CNRS, F-06238 Villefranche-sur-mer, CEDEX, France

Abstract

Optical measurements within both the visible and near ultraviolet (UV) parts of the spectrum (305–750 nm) were recently made in hyperoligotrophic waters in the South Pacific gyre (near Easter Island). The diffuse attenuation coefficients for downward irradiance, $K_d(\lambda)$, and the irradiance reflectances, $R(\lambda)$, as derived from hyperspectral (downward and upward) irradiance measurements, exhibit very uncommon values that reflect the exceptional clarity of this huge water body. The $K_d(\lambda)$ values observed in the UV domain are even below the absorption coefficients found in current literature for pure water. The $R(\lambda)$ values (beneath the surface) exhibit a maximum as high as 13% around 390 nm. From these apparent optical properties, the absorption and backscattering coefficients can be inferred by inversion and compared to those of (optically) pure seawater. The total absorption coefficient (a_{tot}) exhibits a flat minimum (~ 0.007 m^{-1}) around 410–420 nm, about twice that of pure water. At 310 nm, a_{tot} may be as low as 0.045 m^{-1}, i.e., half the value generally accepted for pure water. The particulate absorption is low compared to those of yellow substance and water and represents only $\sim$15% of a_{tot} in the 305–420-nm domain. The backscattering coefficient is totally dominated by that of water molecules in the UV domain. Because direct laboratory determinations of pure water absorption in the UV domain are still scarce and contradictory, we determine a tentative upper bound limit for this elusive coefficient as it results from in situ measurements.

Apart from the inserted quotation mark, the title of this article is identical to that of an article published some 25 years ago by Smith and Baker (1981). This means that perhaps the purest natural waters are not yet discovered and that the subject is still topical. This article is motivated by recent (2004) observations in the exceptionally clear, blue-violet waters of the anticyclonic South Pacific gyre, West of Rapa Nui (Easter Island), and its aims are somewhat similar to those of the Smith and Baker study. Namely, the following questions are addressed: (1) What are the optical properties of these extremely clear natural waters and how can they be explained? (2) Is it possible from their apparent optical properties (AOP) to derive some upper bound limits for the absorption coefficient of pure water? Indeed, laboratory measurements of pure water absorption, particularly in the violet and ultraviolet (UV) part of the spectrum are scarce and contradictory. Somehow paradoxically, it seems that natural waters, in certain conditions (those of extreme oligotrophy), may be purer than those prepared in a laboratory, despite enormous cautions to avoid trace organic impurities. To present their best estimate (upper bound limits) of pure water absorption, Smith and Baker (1981) actually made use of their data in the "clearest" natural waters, namely the freshwater of Crater Lake, Oregon, (Tyler and Smith, 1970) and the seawater of Sargasso Sea (Smith *in* Tyler 1973).

Since Smith and Baker's work, new laboratory determinations of the absorption and attenuation coefficients of carefully purified water have been published. They differ considerably from the previously accepted values, in particular in the (blue-violet) window of maximal transparency (Pope and Fry 1997; Sogandares and Fry 1997), as well as in the UV domain (Quickenden and Irvin 1980; Boivin et al. 1986). Therefore, it is timely to examine the mutual compatibility between these in vitro measurements and the hyperspectral in situ observations, which were made recently in extremely clear waters and encompass both the visible and near UV domains.

The measured increase of UV radiation reaching our planet, with possible consequences upon phytoplankton productivity, aquatic photochemistry, and photobiology or generally upon biogeochemical cycles, stresses the need for a better understanding and prediction of the in-water penetration of short wavelength radiation (*see* e.g., Vasilkov et al. 2005). For this reason, in the present study emphasis will be put on the spectral domain that includes the UVA (400–320 nm), part of UVB (320–280 nm), and blue-violet radiation, a domain where pure water is particularly transparent and its actual transparency is not ascertained.

Study area

Hyperoligotrophic waters with a chlorophyll concentration below 0.03 mg m^{-3} have been systematically detected by ocean color sensors within the vast South Pacific anticyclonic gyre in the vicinity of Easter Island (Claustre

Acknowledgments

The expertise of the captain, officers, and crew of the research vessel, *Atalante*, was an important factor in the success of the BIOSOPE campaign. The authors also acknowledge the valuable comments and suggestions made by two anonymous reviewers.

The financial supports for this cruise of Centre National de la Recherche Scientifique (CNRS) via the Production Océanique et Flux (PROOF) program and additionally from National Aeronautics and Space Administration (NASA) and European Space Agency (ESA) were essential and much appreciated.

and Maritorena 2003). Within the zone delimited by 20–30°S, and 98–122°W, the sea-viewing wide field-of-view sensor (SeaWiFS) data statistically analyzed for the year 1999 (Fougnié et al. 2002) provide an annual mean concentration of 0.032 mg m^{-3}, with a seasonal oscillation from 0.020 in November–January to 0.045 mg m^{-3} in June–August. The Biogeochemistry and Optics South Pacific Experiment (BIOSOPE) cruise (October–December 2004) consisted of an 8,000-km-long transect from the mesotrophic waters near the Marquesas islands through the South Pacific gyre to the eutrophic waters of the Chilean upwelling area (Fig. 1a). An intensive biogeochemical study of this poorly documented hyperoligotrophic and strongly stratified system was a prominent aim of the BIOSOPE cruise. The eight selected stations (*see* Table 1 and Fig. 1b) encompass the zone where the minimal surface chlorophyll values were found; the deep chlorophyll maximum was slightly below the bottom of the euphotic layer and just above the nutricline (1 μmN at ~200 m; P. Raimbault pers. comm.). The thickness of the euphotic layer reached maximal values, often >150 m (defined as that depth where the downward photosynthetic available radiation [PAR] irradiance is reduced to 1% of its surface value; PAR includes the entire 400–700-nm domain).

This hyperoligotrophic zone extends about 3,000 km along the transect and is as wide as the Mediterranean Sea. Near-surface chlorophyll concentration is slightly >0.04 mg m^{-3} at the first and last selected stations and ~ 0.02 mg m^{-3} at the four central stations.

Material and methods

A calibrated spectroradiometer (LI-1800 UW, LI-COR instruments) was used to determine spectrally (from ~305 nm to 800 nm) the planar irradiance at discrete depths. Downward and upward spectral irradiances, $E_d(\lambda,z)$ and $E_u(\lambda,z)$, respectively, were measured around local noon during two separate casts completed in rapid succession using a rotating frame, enabling the instrument to be quickly (within 1–2 min) turned upside down. The data (recorded every 2 nm) were corrected for slight changes in surface solar irradiance during the experiment (duration 30–45 min); solar irradiance was monitored on the deck by a gimbaled cosine collector PAR sensor (PNF, Biospherical Instrument). When doing such a global correction, it is assumed that spectral changes in the incident radiation are insignificant. The $E_d(\lambda,z)$ and $E_u(\lambda,z)$ were all normalized with respect to the same constant spectral incident irradiance. Only the data acquired in good conditions (blue skies, a large portion of blue sky, or completely overcast skies) are considered here. Some stations were abandoned or data discarded because of unfavorable (broken clouds) conditions.

A calibrated pressure sensor enabled the depth of optical measurements to be determined (within 10 cm). The downward irradiance, $E_d(\lambda,0^+)$, was measured above the surface (denoted 0^+), and the irradiance just beneath the surface, $E_d(\lambda,0^-)$, was obtained by applying a neutral coefficient (0.97) for transmission across the air–sea interface. The attenuation coefficient for downward irradiance, $K_d(\lambda)$, is computed (from 0^- to a certain depth z) as

$$K_d(\lambda) = (1/z)\ln(E_d(\lambda,0^-)/E_d(\lambda,z)) \quad (1)$$

The E_d and E_u determinations used to produce the irradiance reflectance, R, are separated in time by a few minutes at most (and are normalized; *see* above); $R(\lambda,z')$, at a certain depth denoted z′, is computed as

$$R(\lambda,z') = E_u(\lambda,z')/E_d(\lambda,z') \quad (2)$$

In Eq. 1, z is the minimal depth enabling $E_d(\lambda,z)$ measurements to be free from noise caused by wave focusing effects, and z is ~ 30–40 m in clear waters with high sun in blue sky or ~ 10–15 m for uniformly overcast skies. The lens effect does not affect upward measurements. Therefore, z′ (in Eq. 2) is the minimal depth (~1.3–2.5 m) that is compatible with swell and a ship's roll. To compute $R(\lambda,z')$, $E_u(\lambda,z')$ is combined with $E_d(\lambda,z')$, which has been extrapolated downward from $E_d(\lambda,0^-)$ by using $K_d(\lambda)$. This procedure provides numerically more stable values of reflectance as compared to those obtained by propagating $E_u(\lambda,z')$ from z′ to 0^-. Besides, $R(\lambda,z')$ and $R(\lambda,0^-)$ are identical (*see* e.g., Morel and Gentili 2004), when z′ is small enough and water is homogeneous at this scale (examples are provided later).

Because K_d and R result from ratios between two irradiance spectra, they are independent from the instrument calibration or drift in calibration during the cruise. The source of inaccuracies is the uncertainty (Δz) that affects the sampling depths z and z′. With $\Delta z/z$ easily controlled within better than 1%, K_d is precisely known and the limitation is only that caused by the above-mentioned focusing effects. Regarding R, the situation is slightly less comfortable because z′ is small, so that $\Delta z'/z'$ can reach 5–10%, and may affect the evaluation of $E_d(\lambda,z')$ (practically in the red part of the spectrum only). Successively repeated experiments, however, have demonstrated that agreement between the derived $R(\lambda)$; better than 4% (10% in the red part of the spectrum), is easily achievable (*see later* Fig. 7).

Water samples were collected (rosette and Niskin bottles) just after the optical deployment. The sampled volumes (11.2 liters in clear waters) were filtered through 25-mm GF/F filters under low vacuum. The absorption spectra of the particles concentrated on the filters were determined from 300 nm to 800 nm according to the glass-fiber technique (Trüper and Yentsch, 1967), and by using a Perkin Elmer (Lambda-19) spectrophotometer. The reference was a wet filter saturated with filtered seawater. The correction for the pathlength amplification effect (the so-called β-effect) was made according to Allali et al. (1997), who developed a specific algorithm for Pacific oligotrophic waters. Absorption spectra of depigmented particles (by applying Kishino et al.'s method) were also determined. For pigment determination, samples (2.8–5.6 liters) were also filtered onto GF/F filters, which were immediately frozen in liquid nitrogen and then stored at −80°C for high-performance liquid chromatography

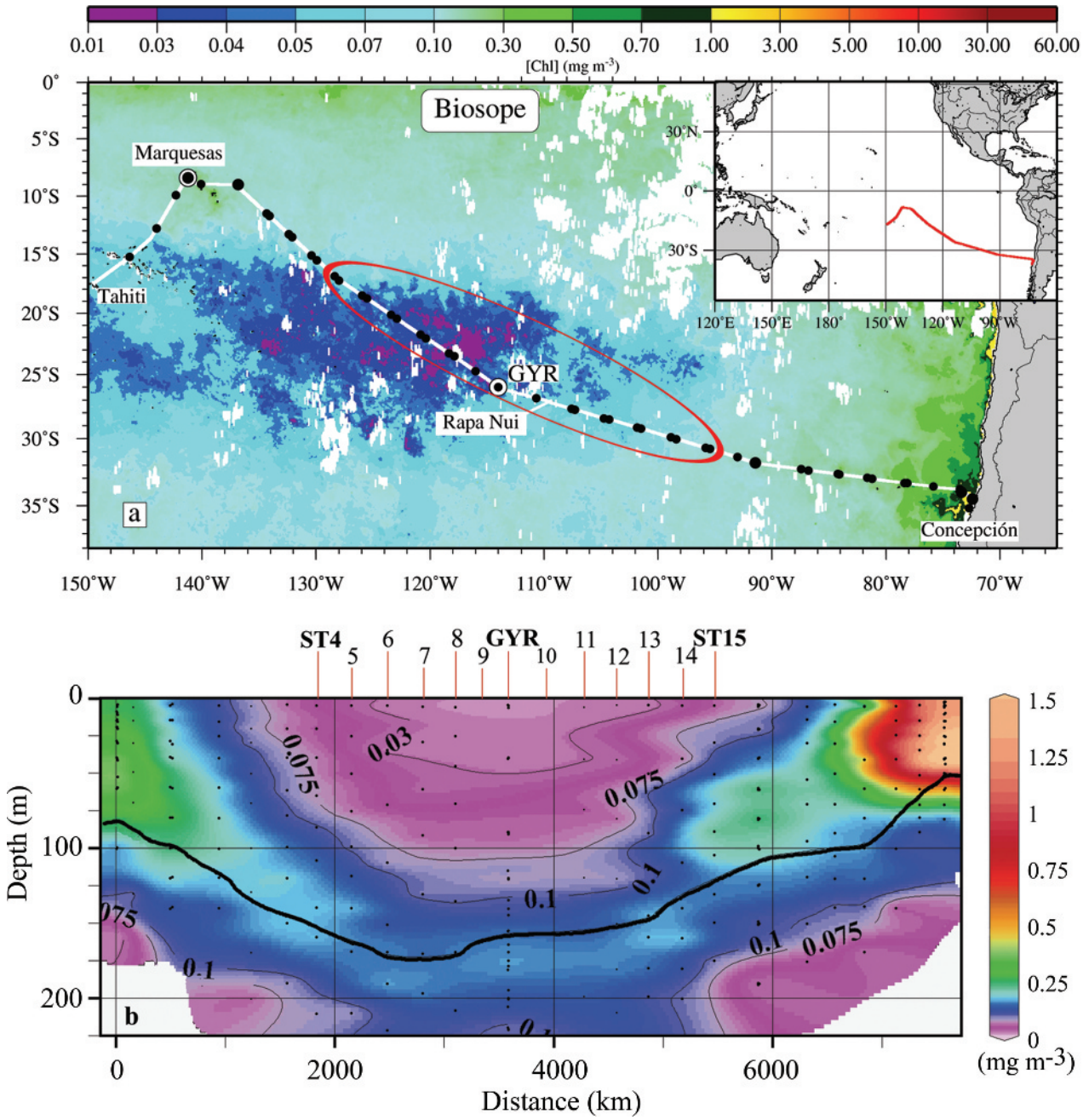

Fig. 1. (a) The transect corresponding to the BIOSOPE cruise is superimposed on a MERIS composite image (level 3) for August 2004, showing the chlorophyll concentration in the upper layer according to a color scale as indicated. The composite for November (the central date of the cruise) has not been used because it is extremely cloudy. It is worth noting that the minimal chlorophyll values are slightly less in August than in November (zone PacSE-6, *in* Fougnié et al. 2004).The clearest stations discussed in the present study are inside the red ellipse. (b) A vertical section (0–250 m) along the transect from Marquesas Islands to the Chilean coastal zone (distance as kilometers), showing the chlorophyll concentration distribution as well as the depth of the euphotic layer (solid black line). The positions of the selected clearest stations (*see* Table 1) are indicated.

(HPLC) analyses in the laboratory. They were made according to a slightly modified version of the method described by Van Heukelen and Thomas (2001; *see* also Hooker et al. 2005). The total chlorophyll *a* (Chl *a*) concentration considered hereafter, denoted as [Chl], is the sum of monovinyl-Chl *a*, divinyl-Chl *a*, and chlorophyllide *a* (the latter is virtually absent in these clear waters).

Results

Downward and upward irradiance spectra (at Station [Sta.] STB 7) are displayed as typical examples for extremely clear waters (Fig. 2). The upper layer of this water body is homogeneous, with [Chl] smoothly increasing from 0.022 mg m^{-3} to 0.032 mg m^{-3} from surface down to

Table 1. Dates and stations selected for the present study of extremely clear waters. The observed quantities include the chlorophyll [Chl] concentration (mg m^{-3}) at two depths within the upper layer; the depth of the euphotic layer (Z_{eu}); the depth of the deep chlorophyll maximum ($Z_{chl\text{-}max}$) with the chlorophyll concentration at this level; the attenuation coefficient K_d at two wavelengths (420 and 310 nm); the particle absorption coefficient, a_p, at two wavelengths (420 and 310 nm); the maximum value of the reflectance spectrum (R_{max}, as %), together with the spectral position of this maximum (λ as nm). The derived quantities include the total absorption coefficient (m^{-1}) at 420 and 310 nm and the absorption coefficients for the dissolved yellow substance (a_{y1}, and a_{y2}, *see* text) at the wavelength 310 nm.

Station	STB-4	STB-5	STB-7	STB-8	GYR-4	GYR-5	STB-14	STB-15
Latitude (°S)	16.52	18.44	22.03	23.33	26.03	26.04	29.55	30.47
Longitude (°W)	128.23	125.57	120.21	117.53	114.01	114.02	98.52	95.25
Year 2004	06 Nov	07 Nov	09 Nov	10 Nov	14 Nov	15 Nov	23 Nov	24 Nov
Observed quantities								
[Chl] (mg m^{-3})								
At 5 m	0.0420	0.0350	0.0220	0.0240	0.0195	0.0200	0.0260	0.0460
At 30–40 m	0.0450	0.0350	0.0200	0.0250	0.0270	0.0250	0.0360	0.0770
Z_{eu} (m)	135	142	172	170	160	166	138	108
$Z_{Chl\text{-}max}$ (m)	160	150	195	175	170	160	155	100
[Chl]-max (mg m^{-3})	0.195	0.204	0.173	0.152	0.178	0.195	0.225	0.247
K_d (420 nm) (m^{-1})	0.0184	0.0170	0.0134	0.0145	0.0120	0.0120	0.0165	0.0230
K_d (310 nm) (m^{-1})	0.0940	0.0810	0.0680	0.0690	0.0700	0.0690	0.0850	0.1150
a_p (420 nm) (m^{-1})	0.0041	0.0038	0.0023	0.0019	0.0022	0.0022	0.0041	0.0054
a_p (310 nm) (m^{-1})	0.0065	0.0045	0.0041	0.0031	0.0055	0.0057	0.0090	0.0120
R_{max} (%)	10.3	11.5	13.5	13.4	13.5	13.3	11.6	10.4
at λ (nm)	390	396	395	394	394	396	396	396
Derived quantities								
a_{tot} (420 nm) (m^{-1})	0.0120	0.0102	0.0072	0.0080	0.0061	0.0064	0.0095	0.0132
a_{tot} (310 nm) (m^{-1})	0.0620	0.0520	0.0410	0.0430	0.0480	0.0430	0.0530	0.0690
a_{y1}(310 nm) (m^{-1})	0.0300	0.0210	0.0070	0.0110	0.0140	0.0120	0.0150	0.0300
a_{y2} (310 nm) (m^{-1})	0.0482	0.0392	0.0252	0.0292	0.0322	0.0202	0.0232	0.0482

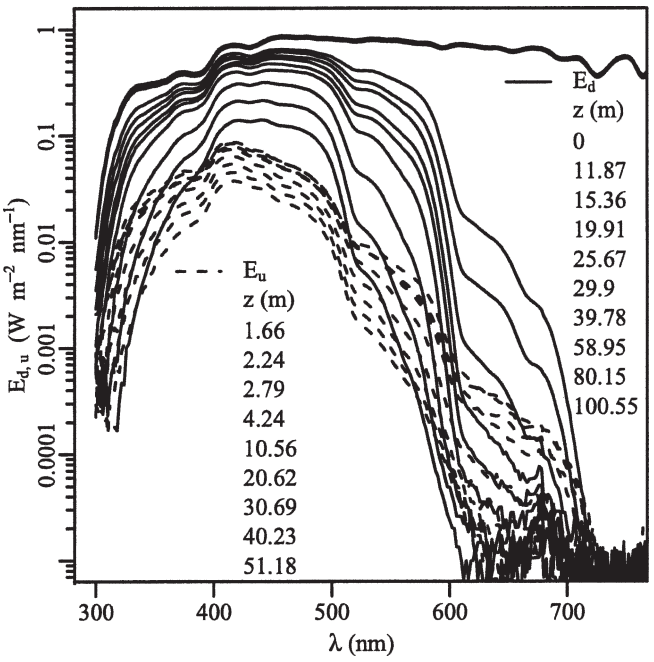

Fig. 2. An example of spectra (Sta. STB-7) of downward and upward irradiance $E_d(\lambda)$ and $E_u(\lambda)$ (logarithmic ordinate scale) determined at discrete depths (m) as indicated. All the spectra are normalized for a constant incident irradiation at the surface and thus are directly comparable (*see* text).

100 m. The [Chl] maximum reached its deepest position (~195 m) at this station (*see* Table 1). At all depths, the near UV upward radiation (330–400 nm) is more intense than the green radiation ($\lambda > 520$ nm). In the red part of the spectrum ($\lambda > 620$ nm), and when the depth increases, the E_d and E_u spectra tend to merge as a result of the dominance of the Raman emission and of the Chl *a* fluorescence signal that emerges from the noise around 685 nm despite the low [Chl] value (discussion in Maritorena et al. 2000).

Diffuse attenuation for downward irradiance

The K_d spectrum for the same station is shown in Fig. 3. The resonance structures typical of the absorption by water molecules are distinctly seen up to the 7th harmonic of the O–H stretch mode occurring near 450 nm (as identified by Pope and Fry 1997). Within the short wavelength domain ($\lambda < 430$ nm), the present K_d values are distinctly below those determined by Tyler and Smith (1970) in Crater Lake (Oregon), renown for its exceptional clarity, and also well below those adopted for the clearest ocean waters by Smith and Baker (1981). They are even below the values these authors proposed for the absorption coefficient, $a_w(\lambda)$. The K_d coefficients for the more transparent water, classified by Jerlov (1976) as Type I, are definitely too high for these Pacific waters and are about twice those we observed in the 310–420-nm range. The spectral shapes also differ, as the K_d minimum (~ 0.013 m^{-1}) is observed at ~ 420 nm, in

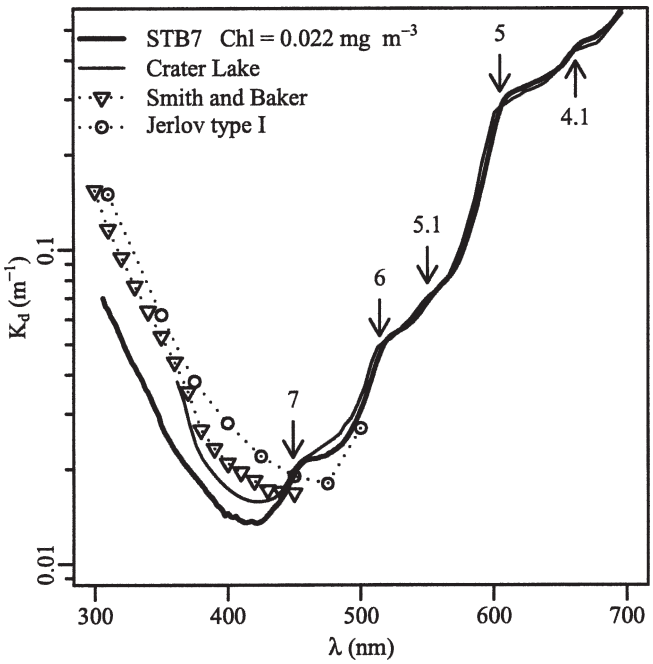

Fig. 3. Diffuse coefficient for downward irradiance, $K_d(\lambda)$, computed between 0^- and 20 m (Sta. STB-7). Also shown for comparison is the spectrum determined in Crater Lake (Tyler and Smith 1970), the $K_d(\lambda)$ values proposed by Smith and Baker (1981) for pure natural waters, and those defining the Jerlov Type I waters. The arrows indicate the position of the (5th, 6th, and 7th) harmonics of the fundamental O–H stretch mode (Pope and Fry 1997), or the combination of the 4th and 5th harmonics with the scissor mode (denoted 4.1 and 5.1).

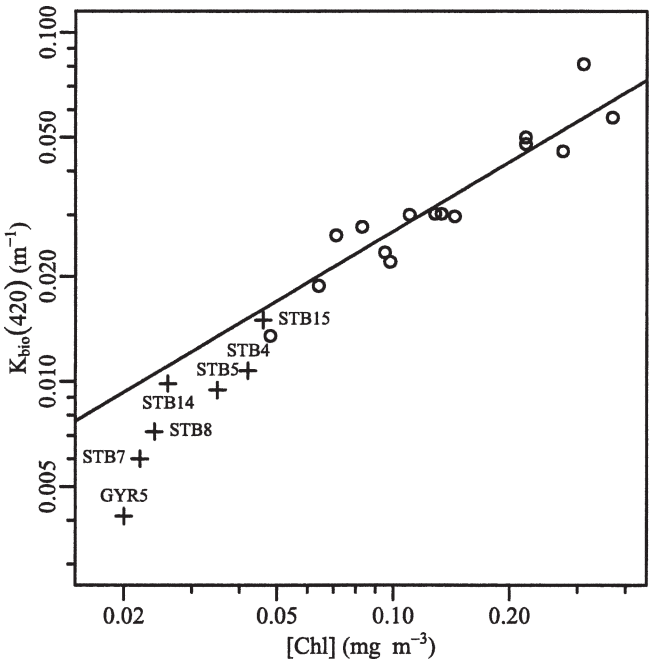

Fig. 5. The fraction of K_d (denoted K_{bio}, *see* text) associated with the presence of particulate and dissolved materials resulting from biological activity as a function of the upper layer chlorophyll concentration. Stations outside the zone of clearest waters (and for [Chl] $>$ 0.045 mg m^{-3}) are also represented (circles). The line corresponds to the empirical relationship proposed by Morel and Maritorena (2001), namely K_{bio} = 0.1227 [Chl]$^{0.659}$. For the lowest [Chl], the K_{bio} values tend to be below the statistical relationship.

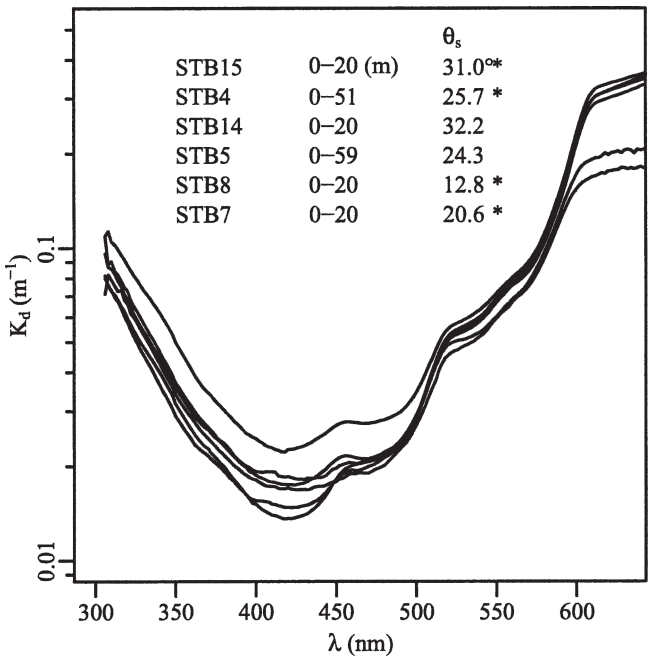

Fig. 4. $K_d(\lambda)$ spectra computed between 0^- and the depths as indicated and for several stations in the clearest waters, from top to bottom (*see* Table 1). The mean zenith-sun angles during the measurements are provided, with an asterisk when the sky was overcast.

agreement with Pope and Fry's findings, whereas in Jerlov's Type I, the minimum (0.018 m^{-1}) is located at 475 nm.

This minimal $K_d(420)$ value is systematically observed for all clear waters sampled (Fig. 4). Nevertheless, these coefficients are still slightly dependent on [Chl] despite the narrow [Chl] range considered. Indeed, when the quantity $K_{bio} = K_d - K_w$ (where K_w is the coefficient for pure water, taken equal to 0.00758 m^{-1}; cf. Morel and Maritorena 2001) is plotted as a function of [Chl], a regular increase in K_{bio} with increasing [Chl] is clearly apparent (Fig. 5).

The $K_d(\lambda)$ values smoothly increase throughout the UVA domain; they still are as low as $\sim$ 0.07 m^{-1} at 310 nm for the four clearest waters (Table 1). For these stations, the $K_d(\lambda)$ values have been averaged across the upper (0–50 m) layer, and these mean values ($\pm$1 SD) are shown in Fig. 6. They are in remarkable agreement with the K_d values published by Vincent et al. (1998) for the ice-covered Lake Vanda (McMurdo dry valleys region, Antarctica), that these authors considered as an "extreme in terms of transparency to solar UV radiation". The similarity in terms of clarity between these two water bodies extends toward the visible domain. Vincent et al. determined a K_{PAR} value of 0.034 m^{-1} (i.e., K_d for the global PAR range), whereas the mean K_{PAR} for the four clearest stations amounts to 0.0352 m^1 ($\pm$0.0025).

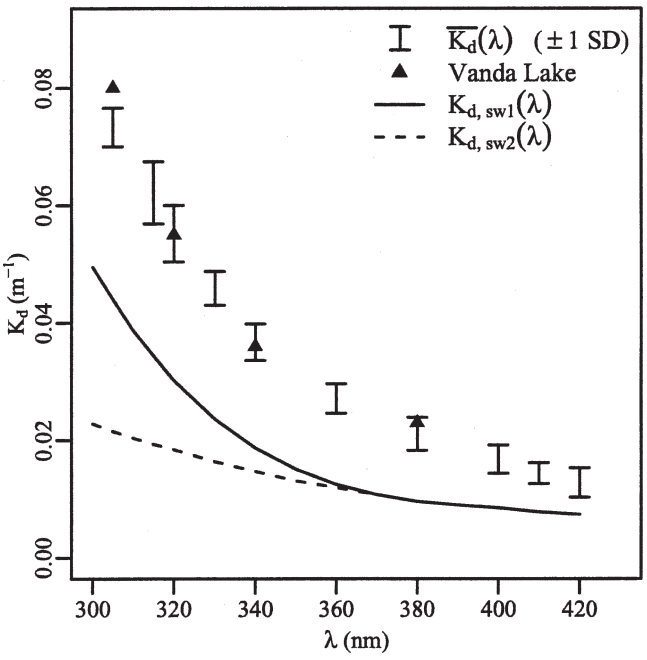

Fig. 6. Averaged $K_d(\lambda)$ values (±1 SD) across the 0–50-m upper layer for the five clearest stations (STB7 and 8, GYR 4, 5a, and 5b) for discrete wavelengths (between 305 nm and 420 nm). Also shown are the four values for Vanda Lake (Vincent et al. 1998) and hypothetic lower limit curves for pure seawater. These values are obtained as in Smith and Baker (1981), according to $K_{d,sw}(\lambda) = a_w(\lambda) + ½\ b_{sw}(\lambda)$, where a_w is either a_{w1} or a_{w2} leading to $K_{d,sw1}$ or $K_{d,sw2}$ (*see* text and Table 2).

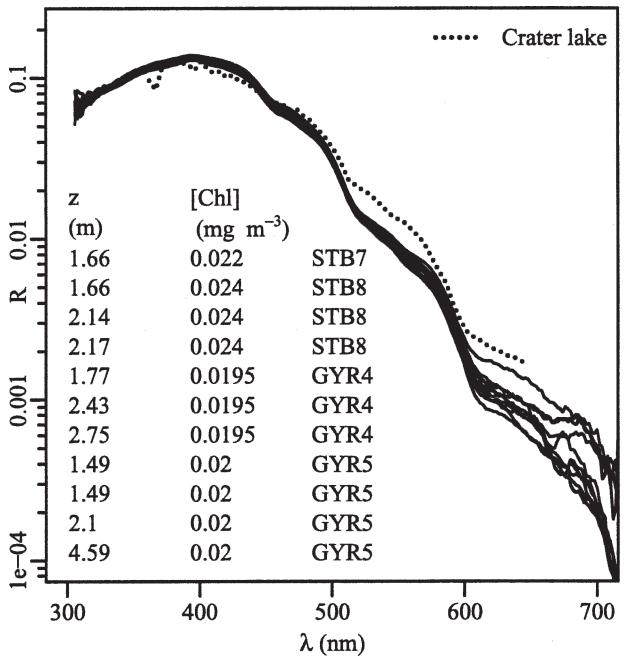

Fig. 7. Reflectance spectra in the near surface layer for all of the clearest waters; stations, depths (z′), and [Chl] are provided. The reflectance spectrum for Crater Lake (Tyler and Smith 1970) is also displayed.

Reflectance

Examples of reflectance spectra in the near surface layer are shown (Fig. 7) for the clearest waters. Between 362 nm and 450 nm, they are slightly above the Crater Lake spectrum (Tyler and Smith 1970). They all exhibit remarkably high R values in the UVB (~6% at 310 nm), and a round maximum exceeding 13% centered on ~394 nm. Between these spectra, subtle nuances exist, which actually are well organized with respect to [Chl]. For instance, ''blue-to-green ratios'', such as R(443) : R(560) and R(490) : R(560), continue to regularly increase when [Chl] decreases within this restricted range of very low concentrations (Fig. 8). The first ratio exceeds 12, and the second ratio is ~ 5.5 when [Chl] < 0.03 mg m^{-3}. Such high values agree with those predicted by the reflectance model of Morel and Maritorena (2001; their Fig. 11).

Analysis

In hydrologic optics, the inverse problem consists of retrieving the inherent optical properties (IOP) from the apparent ones (AOP) (*sensu* Preisendorfer 1961). Various inversion schemes have been recently reviewed by Gordon (2002). The inference of the absorption and backscattering coefficient (a and b_b, respectively) is possible in principle from the knowledge of upward and downward irradiance, or equivalently from K_d and R. The simple inversion developed here is based on the following pair of equations (λ omitted), which also involve two dimensionless quantities, namely μ_d, which is the average cosine of the downward irradiance below the surface, and the factor f′ (Eq. 4 below) which relates R to the IOP.

$$K_d = 1.0395(\mu_d)^{-1}(a + b_b) \tag{3}$$

$$R = f'\,[b_b/(a + b_b)] \tag{4}$$

Both equations were obtained through numerical simulations of the radiative transfer within water bodies (Gordon et al. 1975; Gordon 1989). Equation 3 proved to be very robust in various environmental conditions (*see e.g.*, Morel and Gentili 2004). When solved for a and b_b, the above equations provide the desired inherent coefficients

$$a(\lambda) = 0.962\,K_d(\lambda)\mu_d\,(\theta_s, \lambda, [Chl])\,\{1 - R(\lambda)/f'(\theta_s, \lambda, [Chl])\} \tag{5}$$

$$b_b(\lambda) = 0.962\,K_d(\lambda)\mu_d\,(\theta_s, \lambda, [Chl])\,\{R(\lambda)/f'(\theta_s, \lambda, [Chl])\} \tag{6}$$

Both μ_d and f′ depend on environmental conditions (position of the sun and sky) and on the water optical properties. These quantities have been studied (Morel et al. 2002; Morel and Gentili 2004) for Case 1 waters and varying [Chl] as a function of the zenith sun angle, θ_s in clear blue skies and also for an overcast sky. Lookup tables for μ_d[[Chl], λ, θ_s] and f′ [[Chl], λ, θ_s] have been produced as functions of the three arguments, where [Chl] varies from

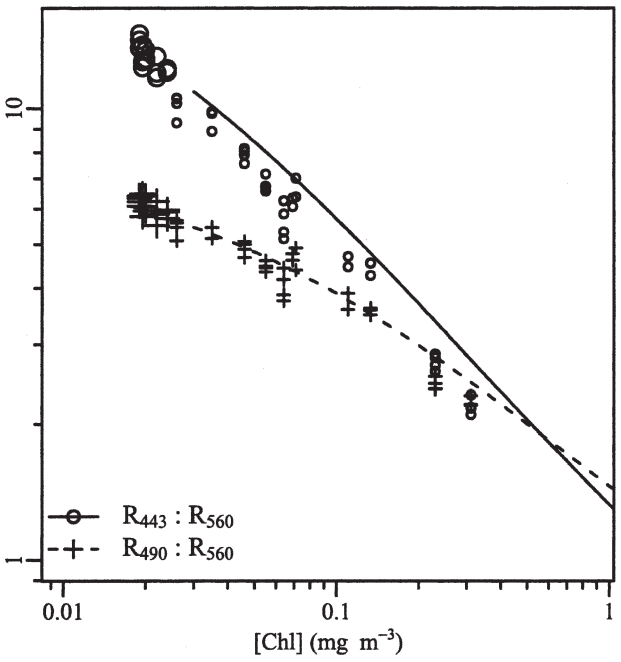

Fig. 8. The ratio of spectral reflectances as indicated, as a function of [Chl], for the clearest waters and for some other waters outside of the hyperoligotrophic zone, also determined during the BIOSOPE cruise. The curves (ocean color algorithms) are those derived from the semi-analytical of Morel and Maritorena (2001, their Figure 11a,b).

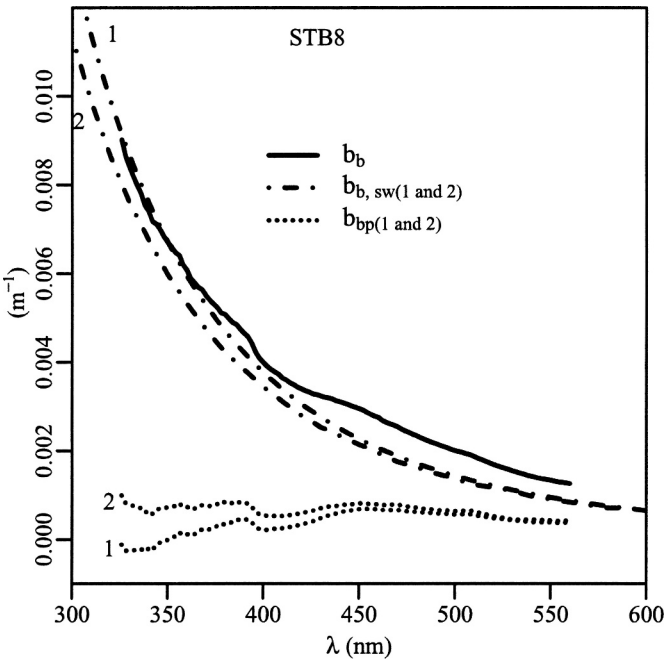

Fig. 9. Example (Sta. STB8) of the inversion providing the backscattering coefficient, $b_b(\lambda)$. Two pure seawater backscattering spectra, $b_{bsw}(\lambda)$, are also displayed (Morel's data [one], Buiteveld et al. data [two]; *see* text). The coefficients for particles $b_{bp1}(\lambda)$ and $b_{bp2}(\lambda)$ are obtained by the difference of $b_{bsw1}(\lambda)$ and $b_{bsw2}(\lambda)$, respectively.

0.02 mg m^{-3} to 10 mg m^{-3}, λ from 350 nm to 700 nm (increment 5 nm), and θ_s from 0° to 75° (increment 15°). They are available on the internet (oceane.obs-vlfr.fr, cd pub/morel, files f, fprime, mud).

The spectral domain considered for this inversion is 310–580 nm, because Raman scattering significantly affects the reflectance and attenuation values beyond 580 nm (*see e.g.*, Haltrin and Kattawar 1991). In contrast, for shorter wavelength domains, the enhancement of reflectance caused by inelastic scattering is very small (e.g., +5% at 400 nm, when [Chl] = 0.03 mg m^{-3}; *see* Fig. 9 in Morel and Gentili 2004). Farther in the UV domain, the Raman emission progressively disappears, because the exciting solar radiation (of shorter wavelength by ~ 40 nm) is vanishingly low and does not reach the sea surface. Emphasis is put on the short wavelength domain where $a_w(\lambda)$ is still inaccurately known. Meanwhile, in the red part of the spectrum, the absorption by the clear waters investigated is practically indistinguishable from that of pure water and does not provide information.

The quality of the retrieved $a(\lambda)$ and $b_b(\lambda)$ coefficients depends on the accuracy of the $K_d(\lambda)$ and $R(\lambda)$ determinations as previously discussed and on that of the tabulated μ_d and f′ values. The latter have been computed by using the IOP of Case 1 waters (Morel and Gentili 2004) as inputs; they are "exact" to the extent that the adopted IOP are representative of the natural environment. These computations were limited to 350 nm in the UV, because of the lack of knowledge regarding the IOPs (particularly of the pure water absorption, a crucial parameter in clear waters). Therefore, the μ_d and f′ values at 350 nm were kept unchanged within the 350–310-nm range for a first inversion. After the adoption of water absorption values (a_{w1}, discussed later), μ_d and f′ were computed for the 350–310-nm range. At λ = 310 nm when [Chl] = 0.02 mg m^{-3} (i.e., in the worst case), they differ from the initial ones by +1.5% for μ_d and by −7% for f′. These new μ_d and f′ values were used for a second inversion.

Backscattering coefficient, $b_b(\lambda)$

An example of the $b_b(\lambda)$ retrieval is provided in Fig. 9. It shows that the inverted spectrum closely follows that of the backscattering coefficient, (b_{bsw}), of pure seawater with its $\lambda^{-4.3}$ spectral dependency. The $b_{bsw}(\lambda)$ theoretical values computed by Morel (1966, 1974) are plotted together with those proposed by Buiteveld et al. (1994). The latter are below (by −8%) Morel's theoretical values, but closer to Morel's experimental determinations (by +4%). The Buiteveld et al. coefficients are multiplied by the factor 1.3 (values in Table 2) to account for the increase of scattering resulting from the presence of salts (Morel 1974).

The preponderance of molecular backscattering is so high in such clear waters that the particle backscattering coefficient cannot be reliably estimated by forming the difference ($b_b(\lambda) - b_{bsw}(\lambda)$). This difference ($<1.10^{-3}$ m^{-1} and sometimes negative) is within the noise inherent to the inversion method combined with the uncertainty of the reflectance determinations. It is even within the limits of

Table 2. Adopted values for the absorption coefficient (m^{-1}) between 300 nm and 500 nm for pure water (cf. Fig. 12), as a function of the wavelength (λ as nm). The column denoted a_{w1} corresponds to the absorption values proposed by Buiteveld et al. (1994), which are based on the attenuation values determined by Boivin et al. (1986) at 254, 313, and 366 nm. The values beyond 420 nm are those of Pope and Fry (1997). A smooth interpolation connects the value of Boivin at 366 nm and that of Pope and Fry at 420 nm. The column denoted a_{w2} corresponds to the absorption values deduced from the attenuation values obtained by Quickenden and Irvin (1980) (between 196 nm and 320 nm). The fitted values (between 300 and 320 nm; *see* Fig. 12) are connected (at 366 nm) to the a_{w1} values. The scattering coefficients (at 20°C) for optically pure seawater, b_{sw} (m^{-1}) are derived from the values proposed by Buiteveld et al. (1994), increased by a factor of 1.30 to account for the presence of salt (at a mean salinity of 36); the backscattering coefficient of pure seawater, b_{bsw} (m^{-1}), is half the scattering coefficient. The attenuation coefficient for downwelling irradiance in hypothetical pure seawater, K_{dsw}, displayed in Fig. 6, is computed according to the approximation (underestimation) $K_{dsw1} = a_{w1} + b_{bsw}$, or $K_{dsw2} = a_{w2} + b_{bsw}$.

λ (nm)	a_{w1} (m^{-1})	a_{w2} (m^{-1})	b_{sw} (m^{-1})	λ (nm)	a_w (m^{-1})	b_{sw} (m^{-1})
300	0.03820	0.01150	0.0226	400	0.00460	0.0069
305	0.03350	0.01100	0.0211	405	0.00460	0.0065
310	0.02880	0.01050	0.0197	410	0.00460	0.0062
315	0.02515	0.01013	0.0185	415	0.00457	0.0059
320	0.02150	0.00975	0.0173	420	0.00454	0.0056
325	0.01875	0.00926	0.0162	425	0.00475	0.0054
330	0.01600	0.00877	0.0152	430	0.00495	0.0051
335	0.01395	0.00836	0.0144	435	0.00565	0.0049
340	0.01190	0.00794	0.0135	440	0.00635	0.0047
345	0.01050	0.00753	0.0127	445	0.00779	0.0044
350	0.00910	0.00712	0.0121	450	0.00922	0.0043
355	0.00810	0.00684	0.0113	455	0.00951	0.0040
360	0.00710	0.00656	0.0107	460	0.00979	0.0039
365	0.00656	0.00629	0.0099	465	0.01011	0.0037
370	0.00602	0.00602	0.0095	470	0.01060	0.0035
375	0.00561		0.0089	475	0.01140	0.0034
380	0.00520		0.0085	480	0.01270	0.0033
385	0.00499		0.0081	485	0.01360	0.0031
390	0.00478		0.0077	490	0.01500	0.0030
395	0.00469		0.0072	495	0.01730	0.0029
				500	0.02040	0.0027

our present knowledge about the pure seawater scattering coefficient.

Total absorption

The absorption obtained through inversion is the total absorption coefficient, a_{tot}, namely, the sum ($a_w + a_p + a_y$) of the absorption coefficients by water, particles, and dissolved yellow substance, respectively. Interpreting a_{tot} ideally requires the knowledge of the three components. The particulate absorption spectra have been determined, but for the two other components, some problems arise. Indeed, (1) the literature values for absorption by pure water, below 420 nm and in the UV domain, are strongly diverging, so that any choice is debatable (*see* discussion below); and (2) in such extremely clear waters, particularly within the upper layer where the yellow substance is partly photodegraded, the experimental a_y values, too close to the detection limit, cannot be safely used.

Regarding $a_y(\lambda)$, however, its well known monotonous increase toward the shorter wavelengths is a piece of information that can serve as a potential constraint in the interpretation of a_{tot} and, therefore, in the inference of a_w. This increase is commonly modeled with an exponential function, such as

$$a_y(\lambda) = a_y(\lambda_0) \exp(-s\,(\lambda - \lambda_0)) \qquad (7)$$

where λ_0 is a reference wavelength. This equation can be used under the proviso that the spectral interval ($\lambda - \lambda_0$) is not too wide, because the exponential slope, s, is not constant within the entire (300–600 nm) spectral range; in particular, s would exhibit higher values in the short wavelength domain (Twardowski et al. 2004).The constraint of continuity would be stringent if the slope was a priori known, which unfortunately is not the case.

The debate about the absorption properties of optically pure water

Upper bound estimates of the absorption coefficient for pure water were inferred by Smith and Baker (1981) from the $K_d(\lambda)$ coefficients observed in very clear natural waters, combined with literature values for $a_w(\lambda)$. The coefficients they proposed for the 200 nm to 800 nm range are still in common use in hydrologic optics. Considerably lower absorptions, however, were later determined by Pope and Fry (1997), from 380 nm to 500 nm. These new values, particularly those within the window of extreme transparency (at ~ 418 nm) proved to account better for the K_d observations in oligotrophic waters (Morel and Maritorena 2001, their Fig. 3).

Data are even more scarce in the UV domain where absorption is expected to be very low. Indeed, this domain corresponds to very high overtones (10–11th) of the fundamental O–H stretch mode (Tam and Patel 1979), and it is far from the tail of the first electronic transition

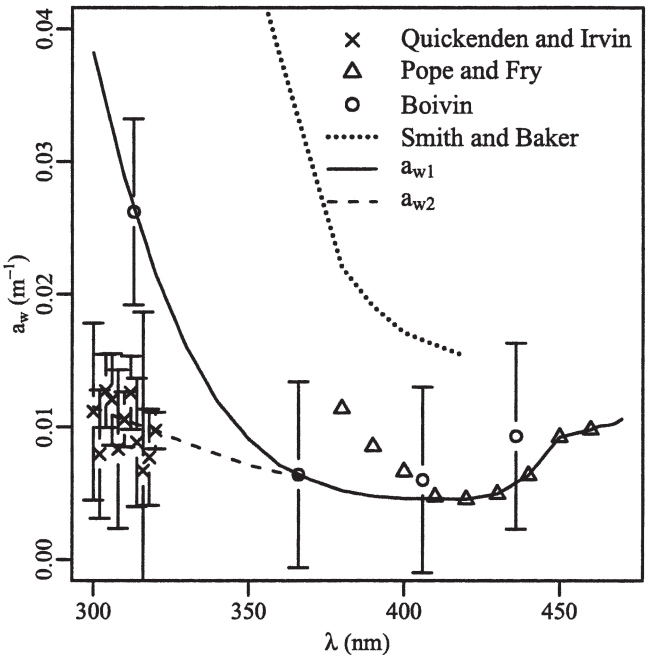

Fig. 10. Historical data of the absorption coefficient by pure water in the blue and UV part of the spectrum. The dotted curve represents (part of) the values proposed by Smith and Baker; the triangles are those of Pope and Fry. The vertical bars represent the 50% confidence interval around the mean of three determinations at each wavelength by Quickenden and Irvin (crosses) or the estimated uncertainty for the data of Boivin et al. (circles; their value at 254 nm is not shown). The curve denoted a_{w1} is obtained by using the Boivin et al. data (as interpolated from 300 nm to 370 nm by Buiteveld et al.) and by connecting the value at 370 nm to the Pope and Fry data at 410–420 nm. The curve a_{w2} results from an extrapolation of the Quickenden and Irvin data (between 300 nm and 320 nm) toward Boivin's datum at 366 nm (*see* Table 2). Beyond 366 nm, a_{w1} and a_{w2} are identical.

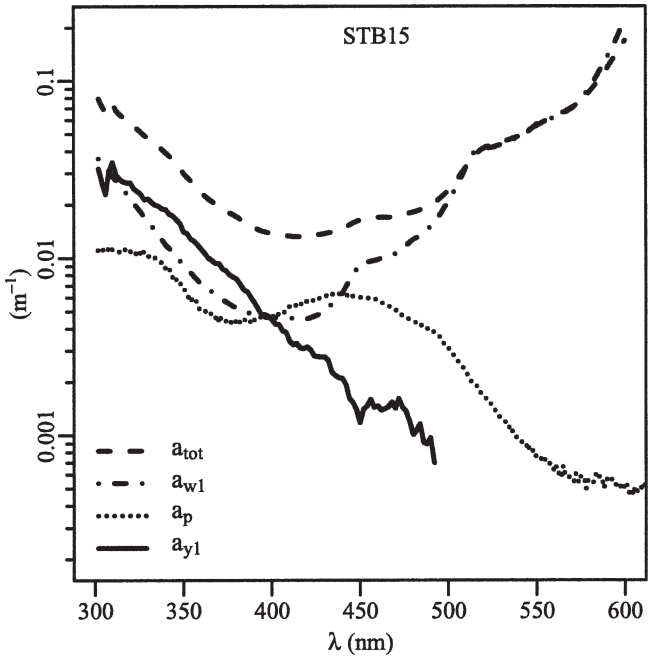

Fig. 11. Example (Sta. STB 15) of the inversion providing the absorption coefficients, denoted a_{tot}, in the 305–600-nm interval. The measured absorption spectrum, a_p, of the particulate material is also displayed; the absorption spectrum of yellow substance, a_{y1}, is derived by using the a_{w1} curve of Fig. 10.

bands occurring below 150 nm. Measurements of the (beam) attenuation coefficients of carefully purified water were published by Quickenden and Irvin (1980, for the 196–320 nm domain, 1-nm step), and by Boivin et al. (1986, for five discrete wavelengths, from 254 nm to 578 nm). A differential pathlength method was employed with 1- and 10-cm-long cells (net pathlength 9 cm; Quickenden and Irvin's study) or a conventional method with a unique 50-cm-long cell (Boivin et al. 1986) was used. Despite their uncertainties and divergences, both of these studies result in attenuation values near 300 nm well below those previously available. The scattering coefficient by water molecules, $b_w(\lambda)$ (the major contributor to the attenuation in the UV), is subtracted from the attenuation coefficients, $c_w(\lambda)$, to obtain a_w. After this subtraction is made, the resulting two sets of $a_w(\lambda)$ values (Fig. 10) considerably differ.

The a_w values, derived from Boivin et al. (as interpolated by Buiteveld et al. 1994) and from Quickenden and Irvin determinations, are smoothly connected (at 410 nm) with those of Pope and Fry to obtain the curves a_{w1} and a_{w2}, respectively. These two curves (Fig. 10 and Table 2), which split off below 370 nm, will be used in parallel in the next discussion. Note that the ionic species or dissolved gases present in seawater are believed to be non-absorbing in the spectral range considered here.

Components of absorption

An example of inversion providing $a_{tot},(\lambda)$ is displayed in Fig. 11 together with the a_{w1} spectrum. Within the 400–310-nm range, these values are below the pure water absorption values of Smith and Baker (1981). Beyond 520 nm, the a_{tot} and a_{w1} curves practically merge; in contrast, they progressively diverge in the short wavelength domain, leaving room for other kinds of absorption. The particulate absorption spectrum $a_p(\lambda)$ at this station (sampling depth 5 m) is also displayed. In addition to the usual peak around 445 nm, the spectral shape is characterized by a pronounced minimum around 365 nm and then by an increase toward the UV; note that $a_p(330)$ is about twice the $a_p(445)$ value at the blue peak, and this $a_p(330)$ value is equally shared by phytoplankton and detritus (not shown). This spectral shape, with small nuances, is common to all of our clear stations. The a_p increase between 365 nm and 300 nm likely reveals the presence of mycosporine-like amino acids (Morrison and Nelson 2004), but not in a considerable concentration (no distinct peak around 320 nm, observed in some other stations). The a_p values are much smaller than the a_{tot} values (by a factor ~5 at 400 nm and a factor ~10 at 310 nm). Owing to this disproportion between a_p and a_{tot}, the uncertainty about the pathlength amplification correction (rather unknown in the UV domain) cannot significantly affect the estimate of the other components. Consequently, in the UV domain, the residual and

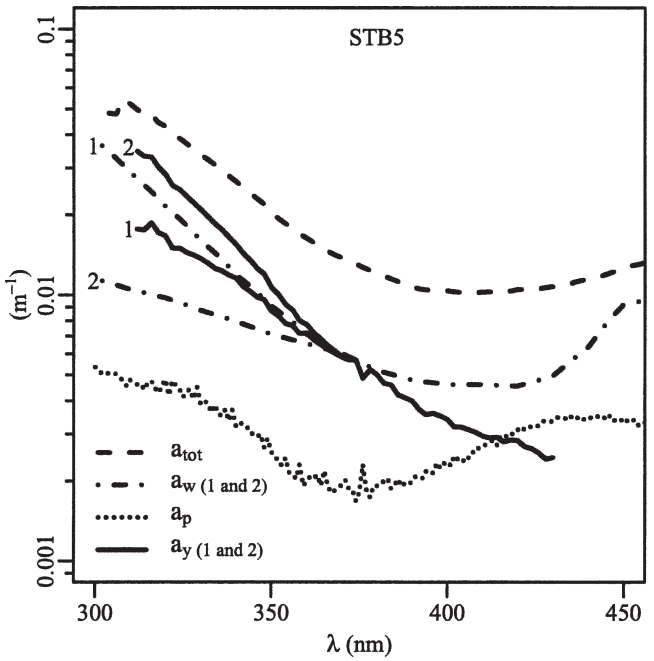

Fig. 12. Example as in Figure 11 (but for Sta. STB5) and with two spectra for the yellow substance, a_{y1} and a_{y2}, derived by using either the a_{w1} or the a_{w2} curves for pure water from Fig. 10. Note that the a_{y1} and a_{y2} spectra diverge only in the 305–370-nm domain.

relatively large quantity, $[a_{tot},(\lambda) - a_p\ (\lambda)]$, is to be shared only by the two unknown components, namely water and yellow substance.

The yellow substance spectrum, obtained as $a_{y1}\ (\lambda) = a_{tot}(\lambda) - a_p\ (\lambda) - a_{w1}(\lambda)$, is shown in Fig. 11. When approaching 500 nm, $a_{y1}(\lambda)$ is numerically unstable, with values <0.001 m^{-1}. Between 500 nm and 310 nm, the $a_{y1}(\lambda)$ spectrum exhibits a rather regular ascending slope (s = 0.0203, computed between 480 nm and 310 nm). At 310 nm, water molecules and yellow substance contribute equivalently to a_{tot}, with a common value about three times that of a_p. At 400 nm, the three components play equal roles in forming a_{tot}. At 420 nm, a_p slightly exceeds a_w, whereas at 450 nm and beyond, water is definitely the dominant contributor.

The retrieval of $a_y(\lambda)$ can also be made by using the $a_{w2}(\lambda)$ curve (denoted a_{y2}), and an example (Sta. STB5, where the lowest a_p values were observed) is shown in Fig. 12. Because the total absorption is extremely low at these stations, the extraction of a_y becomes particularly sensitive to the choice made for a_w. There is clearly a slope change at 370 nm in the a_{y2} spectrum that does not appear in the a_{y1} spectrum. When computed between 370 nm and 308 nm, the slope s is 0.0317 or 0.0198 nm^{-1} for a_{y2} or a_{y1}, respectively, whereas the common slope is ~ 0.0178 nm^{-1} between 370 nm and 420 nm.

More generally, for the eight oligotrophic stations leading to 18 a_{tot} separate inversions, the average s-slope (nm^{-1}) between 310 nm and 370 nm (N = 18) is either 0.0332 ($\pm$0.0033 at 1 SD), or 0.0203 ($\pm$0.0025), when the a_{w2} or a_{w1}curves are used to produce the a_y spectra. Between 370 nm and a variable upper limit (ranging from 380 nm to 420 nm, according to the reliability of the a_y retrieval), the slope value amounts to 0.0210 ± 0.0035 (N = 14), i.e., a value thay is roughly in continuity with the second value above (0.0203 ± 0.0025).

Southeast of Bermuda in oligotrophic waters comparable to those of the South Pacific (even if slightly less clear), the mean slope value in the UV computed between 280 nm and 350 nm amounts to 0.0235 ($\pm$0.0025) nm^{-1} (Nelson et al. 1998). At the surface layer (1–20 m) at the same location, the slope between 320 nm and a wavelength corresponding to the detection limit was seasonally varying between 0.0152 nm^{-1} (minimum in winter) and 0.0194 nm^{-1} (maximum in autumn) (Nelson et al., 2004). A rather high s-value (0.034 nm^{-1}, apparently for the 290–330-nm domain, was reported by Green and Blough (1994) in the Gulf of Mexico. The magnitude of yellow substance absorption in these locations is considerably higher than in the southeast Pacific. The minimal $a_y(300)$ values are ~ 0.15 m^{-1} (Nelson et al. 1998), or 0.10 m^{-1} (at 337 nm, Green and Blough 1994), whereas for the four central stations, the a_y (310) values remain well below 0.03 m^{-1} (Table 1).

Discussion

More insight can be gained by considering clear waters other than the clearest ones. With increasing [Chl], $a_y(370)$ increases rather regularly (Fig. 13). The $a_{y,1}$ and $a_{y,2}$ branches (in the 310–370-nm range) become less distinct, because the relative contribution of a_w to a_{tot} is declining in such "less clear" waters. When stations outside of the hyperoligotrophic gyre (with [Chl] $<$ 0.37 mg m^{-3}) are considered, the upper limit for the retrieval of a_y can be pushed up to 440–460 nm. When merging these additional stations with those of the hyperoligotrophic zone, the general slope within the 370–400 (occasionally 460) nm interval amounts to 0.0164 ± 0.0044 nm^{-1} (with N = 32). For the 310–370-nm interval the slopes are 0.0276 ± 0.0036 for a_{y2} and 0.0191 ± 0.0027 for a_{y1}. If the difference in slope persists, it tends to decline. These results (normalized at 370 nm) are summarized by Fig. 14.

In summary, the argument of a smoother continuity for the a_y slope is in favor of the Boivin et al. absorption values in the UV domain. It is not irrefutable, however. Indeed, a curvature in the log-transform representation of a_y is known to exist, with steeper slopes toward the UV domain (Twardowski et al. 2004). Photo-bleaching may also induce a slope change, as well as microbial production of colored dissolved organic matter (Nelson et al. 2004). Slope values (inside the UV domain and its subdomains) are not presently well documented, in large part because of the difficulty of preparing an ultrapure water standard assuredly exempt from organic impurities. When data are available, they generally correspond to waters with a much higher yellow substance content [recall that the present $a_y(412)$ values are of the order of 0.002 m^{-1}]. Therefore, it could be argued that the very small amount of yellow substance present in this part of the ocean might differ in its nature from what was measured elsewhere. It is worth remarking that water absorption values higher than those

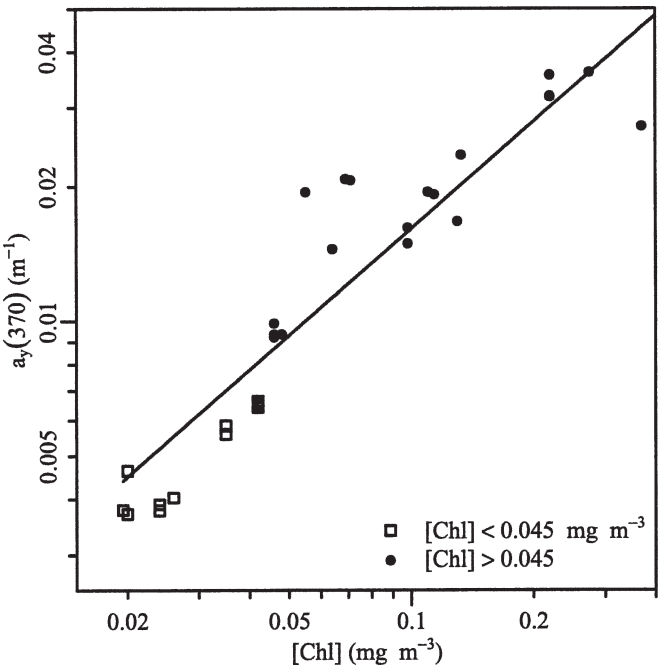

Fig. 13. Absorption coefficient at 370 nm of the yellow substance, plotted as a function of [Chl] for the clearest waters of the BIOSOPE cruise (squares, [Chl] < 0.045 mg m^{-3}) and for waters at the periphery of the hyperoligotrophic zone (dots, $0.045 <$ [Chl] < 0.4 mg m^{-3}). The straight line corresponds to the best fit, which expresses as $a_y(370) = 0.100$ [Chl] $^{0.80}$ ($r^2 = 0.94$).

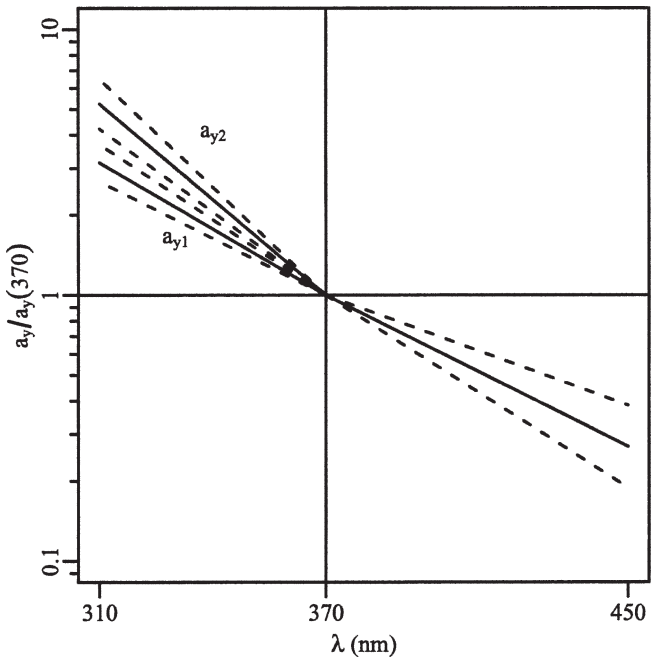

Fig. 14. Averaged slopes (solid lines, ± 1 SD, dashed lines) in the 310–370 nm domain when using the a_{y1} and a_{y2} values and beyond 370 nm, the common unique averaged slope, (also with ± 1 SD, dashed lines).

of Boivin-Buiteveld (i.e., a_{w1}) would lead to an inverted bending, i.e. to s-slopes smaller in the 370–310-nm domain than in the adjacent 370–450-nm domain, which is very unlikely.

The a_{w1} values can provisionally be considered as a reasonable limit for pure water absorption in the UV domain. Recent determinations of water absorption in the 360–300 nm domain (Fry and Lu, pers. comm.), still slightly above those of Boivin, tend to confirm them. In the intermediate domain (370–420 nm), the interpolated a_{w1} spectrum enables smooth a_y spectra to be derived (Figs. 11, 12). This smoothness would be not possible if the Pope and Fry absorption values (markedly increasing toward 380 nm) were used, which casts some doubts on their previous determinations in this domain. In contrast, their extremely low values around 417.5 nm account very well for the minimal K_d values observed in the clearest waters.

It is common practice to believe that the lowest a_w values are the best ones, as a consequence of a better purification. From this viewpoint, the Quickenden and Irvin purification process is extremely sophisticated. Yet, with an effective pathlength of 9 cm their measurements in the 300–320 nm range are too close to the detection limit to be fully reliable. This is clearly evidenced by the dispersion of the attenuation values and associated errors (actually some attenuation values lead to negative absorption). New in vitro measurements are definitely needed to pinpoint the true water absorption in UV. The present attempts to at least fix upper bound limits from in situ determinations find their justification in the present lack of knowledge.

These South Pacific waters are nearly identical to the purest freshwater observed in an Antarctic desert lake, and when compared to other oceanic waters, they also appear to be the clearest ones ever sampled. Indeed, in our collection of data, the only one resembling the situation is that found in the South-East Sargasso Sea (Discoverer, Sta. 21, 25°45N–65°40, June 1, 1970; *in* J. Tyler 1973). With a deep [Chl] maximum (0.2 mg m^{-3}) at 120 m (Z_{eu} at 116 m), near-surface [Chl] ~ 0.027 mg m^{-3}, R(443)/R(560) $\sim 9\%$, and $K_d(420) \sim 0.0194$ m^{-1}, this water was almost as pure and "violet-blue" as those near Easter Island. Plotted within the CIE-1957 chromaticity diagram, the near-surface reflectance spectra lead to a dominant color centered on 473 nm with a purity of 81% for the Sargasso Sea and on 470–471 nm with a purity of 80% for the clearest BIOSOPE stations. Although renowned for their clarity, the East Mediterranean waters (with [Chl] = 0.023 mg m^{-3}, Sta. 17b, the clearest one of the Minos cruise), are significantly less transparent than those of the Pacific, particularly in the near UV domain (as already shown in Fig. 7 in Morel and Maritorena 2001). In this reference (Fig. 10a), data for a station in the tropical Pacific were already presented (16°S–150°W, with [Chl] = 0.045 mg m^{-3}, Z_{eu} 132 m, 25–27 November, 1994, OLIPAC cruise). The clearest waters of this cruise are almost identical to those observed at the periphery of the hyperoligotrophic zone (Sta. STB 4 and 15) and hence, are definitely less clear than those in the center.

According to an analysis of the SeaWiFS ocean color data, oligotrophic conditions, with [Chl] close to

0.02 mg m^{-3} and high blue reflectance, also prevail in the northwest Pacific (around 15°N–165°E; Fougnié et al. 2002). Thus, other instances of extreme transparency, similar to those of Easter Island, could be found there, and perhaps also within other oligotrophic subtropical gyres, unaffected by winter vertical mixing. Nevertheless, the exceptional size of the South Pacific gyre compared to other subtropical gyres is probably favorable to the formation of a huge reservoir of such extraordinary clear waters.

The depth of the euphotic layer (the present Z_{eu} values, about 170 m, are the deepest ever reported) is often adopted as a global (i.e., polychromatic) criterion for clarity. Yet, the deep chlorophyll maximum, which generally encroaches upon the deepest layers of the euphotic zone, reduces Z_{eu} accordingly; therefore, this depth is not the appropriate descriptor of the transparency of the upper layers. Beside, Z_{eu}, only related to the penetration of visible radiation, is, by definition, insensitive to the UV penetration; the discriminating tool, available when considering the UV domain, is thus unemployed. Actually, absorption in this spectral domain is the most sensitive criterion to evaluate the degree of clarity in natural waters. At least below a certain minimal [Chl] level, particulate matter (phytoplankton and retinue) has a minor impact on absorption (Fig. 12). This fact was already noted for the Sargasso Sea by Nelson et al. (1998). As a consequence, the changes in yellow substance content become the dominant cause of residual optical variations (*see* e.g., Siegel et al. 2002, 2005), and the degree of clarity is more accurately characterized by UV absorption coefficients.

Finally, it remains somewhat surprising that it is possible to observe in the natural environment an enormous reservoir with such a low content of UV-absorbing substances, while it is so difficult in the laboratory to prepare water samples deprived of organic impurities. In subtropical gyres, the reduced diffusive fluxes of nutrients and dissolved organic material from depth, combined with a high irradiance, generate a correlation between [Chl] and yellow substance (Siegel at al. 2005). Such conditions are in their extremes in the South-Pacific gyre. The huge size of this gyre, the distance from terrestrial sources of volatile organic compounds, the residence time of these quiescent waters accumulated inside the anticyclonic circulation, the depth of the nutricline, and thus the strongly nutrient-limited photosynthetic activity, when combined with an exposition to strong photodestructive UV radiation, are likely to be the origin of this paradoxical water purity.

References

Allali, K., A. Bricaud, and H. Claustre. 1997. Spatial variations in the chlorophyll-specific absorption coefficients of phytoplankton and photosyntheticaly active pigments in the equatorial Pacific. J. Geophys. Res. **102:** 12413–12423.

Boivin, L. P., W. F. Davidson, R. S. Storey, D. Sinclair, and E. D. Earle. 1986. Determination of the attenuation coefficient of visible and ultraviolet radiation in heavy water. Appl. Opt. **25:** 188–192.

Buiteveld, H., J. H. M. Hakvoort, and M. Donze. 1994. The optical properties of pure water. SPIE Ocean Optics XII **2258:** 174–183.

Fougnié, B., P. Henry, A. Morel, D. Antoine, and F. Montagner. 2002. Identification and characterization of stable homogeneous oceanic zones: Climatology and impact on in-flight calibration of space sensor over Rayleigh scattering. Ocean Optics XVI, Santa Fe, NM.

Gordon, H. R. 1989. Can the Lambert-Beer law be applied to the diffuse attenuation coefficient of ocean water? Limnol. Oceanogr. **34:** 1389–1409.

———. 2002. Inverse methods in hydrologic optics. Oceanologia **44:** 9–58.

———, O. B. Brown, and M. M. Jacobs. 1975. Computed relations between inherent and apparent optical properties of a flat homogeneous ocean. Appl. Opt. **14:** 417–427.

Hooker, S. B., and others. 2005. The second SeaWiFS HPLC analysis round-robin experiment (SeaHARRE-2). NASA/TM **212785:** 1–110.

Kishino, M., M. Takahashi, N. Okami, and S. Ichimura. 1985. Estimation of the spectral absorption of phytoplankton in the sea. Bull. Mar. Sci. **37:** 634–642.

Maritorena, S., A. Morel, and B. Gentili. 2000. Determination of the fluorescence quantum yield by oceanic phytoplankton in their natural habitat. Appl. Opt. **39:** 6725–6737.

Marshall, B. R., and R. C. Smith. 1990. Raman scattering and in-water ocean optical properties. Appl. Opt. **29:** 71–84.

Morel, A. 1966. Etude expérimentale de la diffusion de la lumière par l'eau, les solutions de chlorure de sodium, et l'eau de mer optiquement pures. J. Chim. Phys. **10:** 1359–1366.

———. 1974. Optical properties of pure water and pure seawater, p. 1–24. *In* N. G. J. E. Steeman-Nielsen [ed.], Optical aspects of oceanography. Academic.

———, D. Antoine, and B. Gentili. 2002. Bidirectional reflectance of oceanic waters: accounting for Raman emission and varying particle scattering phase function. Appl. Opt. **41:** 6289–6306.

———, and B. Gentili. 2004. Radiation transport within oceanic (case 1) waters. J. Geophys. Res. **109:** C06008, doi:10.1029/2003JC002259.

———, and S. Maritorena. 2001. Bio-optical properties of oceanic waters: A reappraisal. J. Geophys. Res. **106:** 7163–7180.

Morrison, L. R., and N. B. Nelson. 2004. Seasonal cycle of phytoplankton UV absorption at the Bermuda Atlantic Time-series Study (BATS) site. Limnol. Oceanogr. **49:** 215–224.

Nelson, N. B., C. A. Carlson, and D. K. Steinberg. 2004. Production of chromophoric dissolved organic matter by Sargasso Sea microbes. Mar. Chem. **89:** 273–287.

———, D. A. Siegel, and A. F. Michaels. 1998. Seasonal dynamics of colored dissolved material in the Sargasso Sea. Deep-Sea Res. I **45:** 931–957.

Pope, R. M., and E. S. Fry. 1997. Absorption spectrum (380–700 nm) of pure water, II, integrating cavity measurements. Appl. Opt. **36:** 8710–8723.

Preisendorfer, R. W. 1961. Application of radiative transfer theory to light measurement in the sea. IUGG Monography **10:** 11–30.

Quickenden, T. I., and J. A. Irvin. 1980. The ultraviolet absorption of liquid water. J. Chem. Phys. **72:** 4416–4428.

Siegel, D. A., S. Maritorena, N. B. Nelson, and M. J. Behrenfeld. 2005. Independence and interdependencies among global ocean color properties: Reassessing the bio-optical assumption. J. Geophys. Res. **110:** C07011, doi: 10.1029/2004JC002527.

———, ———, ———, D. A. Hansell, and M. Lorenzi-Kaiser. 2002. Global distribution and dynamics of colored dissolved and detrital organic materials. J. Geophys. Res. **107(C12):** 3228, doi:10.1029/2001JC000965.

Smith, R. C., and K. S. Baker. 1981. Optical properties of the clearest natural waters (200–800 nm). Appl. Opt. **20:** 177–184.

Sogandares, F. M., and E. S. Fry. 1997. Absorption spectrum (340–640 nm) of pure water. I. Photothermal measurements. Appl. Opt. **33:** 8699–8709.

Tam, A. C., and C. K. N. Patel. 1979. Optical absorptions of light and heavy water by laser optoacoustic spectroscopy. Appl. Opt. **18:** 3348–3358.

Trüper, H. G., and C. S. Yentsch. 1967. Use of glass-fiber filters for the rapid preparation of in vivo absorption spectra of photosynthetic bacteria. J. Bact. **94:** 1255–1256.

Twardowski, M. S., E. Boss, J. M. Sullivan, and P. L. Donaghay. 2004. Modeling the spectral shape of absorption by chromophoric dissolved organic matter. Mar. Chem. **89:** 69–48.

Tyler, J. E. 1973. Data Report SCOR Discoverer Expedition (May 1970). University of California, Scripps Institution of Oceanography.

———, and R. C. Smith. 1970. Measurements of spectral irradiance underwater. Gordon & Breach science publishers.

Vasilkov, A. P., J. R. Herman, Z. Ahmad, M. Kahru, and B. G. Mitchell. 2005. Assessment of the ultraviolet radiation field in ocean waters from space-based measurements and full radiative-transfer calculations. Appl. Opt. **44:** 2863–2869.

Vidussi, F., H. Claustre, B. B. Manca, A. Luchetta, and J. C. Marty. 2001. Phytoplankton pigment distribution in relation to upper thermocline circulation in the eastern Mediterranean Sea during winter. J. Geophys. Res. **106:** 19,939–19,956.

Vincent, W. F., R. Rae, I. Laurion, C. Howard-Williams, and J. C. Priscu. 1998. Transparency of Antarctic ice-covered lakes to solar UV radiation. Limnol. Oceanogr. **43:** 618–624.

Received: 15 March 2006
Accepted: 28 July 2006
Amended: 7 August 2006